

# RECONFIGURABLE ANTENNAS AND RF FRONT ENDS FOR PORTABLE WIRELESS DEVICES

David T. Auckland, Shawn D. Rogers (Etenna Corporation, Laurel, MD, [dauckland@etenna.com](mailto:dauckland@etenna.com), [srogers@etenna.com](mailto:srogers@etenna.com))  
James T. Aberle (Arizona State University, Tempe, AZ, [aberle@asu.edu](mailto:aberle@asu.edu))

## ABSTRACT

There is tremendous demand for antennas with high efficiencies in very small form factors that fit inside portable wireless devices like handsets and PDAs. These antennas must cover a variety of frequency bands and support different wireless standards. The state-of-the-art in existing handsets appears to be internal antennas that occupy volumes of 4500 to 8000 mm<sup>3</sup>, offer tri-band coverage (GSM, PCS & DCS), and have radiation efficiencies of 10% (in-situ) to 60% (free space). Covering additional bands with a single antenna having enough efficiency and bandwidth is a major challenge. One possible solution to this problem is to use reconfigurable antennas that tune to different frequency bands and have enough instantaneous bandwidth and efficiency for each. Such an antenna would not cover all bands simultaneously, but provides narrower instantaneous bandwidths that are dynamically selectable at higher efficiency than conventional antennas. Such tunable antenna technology is an enabler for software definable radios (SDR) whose RF front ends and even integrated circuits must be reprogrammable on the fly. This paper discusses the practical implementation issues, limitations, and measured results of small, narrowband, tunable antennas within portable handsets.

## 1. INTRODUCTION

The evolution of handset technology to multi-mode, multi-band, and multi-functional designs is in part due to the desire to provide greater and more seamless coverage across the globe (e.g., the “world phone”) and to provide greater choice of functionality to the customer. This trend will eventually culminate with the realization of SDR handsets. The progression towards SDR handsets will give rise to many generations of radio transceiver architectures, each providing greater functionality, higher levels of integration, and enhanced performance. The rate of evolution in transceiver architecture is influenced significantly by advancements in front end component

technology including packaging and integration issues associated with RF passives such as filters, switches, duplexers, and diplexers. To date, a critical element of the front end, namely the antenna, has not been fully exploited as a key SDR enabler. Not only does the antenna play an important role in the evolution towards SDR, but the exploitation of certain properties of the antenna, such as dynamically controlling its frequency response, can actually accelerate the implementation and adoption of SDR handset designs.

The gain-bandwidth limitation of electrically small antennas is a fundamental law of physics that determines the ability of the wireless system engineer to simultaneously reduce the antenna’s footprint while increasing its bandwidth and efficiency. The tradeoff between an antenna’s radiation efficiency ( $\eta$ ), its 3dB bandwidth ( $\beta$ ), and its size ( $a$ ) is well known [1] when the antenna is electrically small ( $a \ll \lambda$ ). The curves in Figure 1 illustrate the maximum efficiency-bandwidth product versus size that is achievable regardless of the matching network used. The spherical curve is the theoretical best because it represents a perfectly matched lowest order spherical mode at a diameter of  $a/\lambda$ . The circular aperture

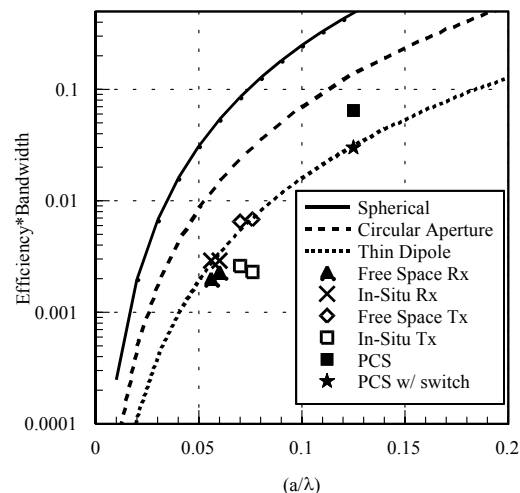


Figure 1. Efficiency-bandwidth versus antenna size.

[2] is for a TE<sub>01</sub> mode in an infinite ground plane. The dipole gives the worst result of the three but it uses the least amount of the spherical volume available. The y-axis value of each curve is antenna fractional bandwidth if the antenna is 100% efficient. Real world effects, such as proximity to a human body or lossy components in a handset will reduce the efficiencies at which certain bandwidths can be obtained. A number of measured data points for actual antennas are shown on the plot and will be discussed later in the paper.

When one carefully reflects on the requirements for a wireless system, one realizes that the ideal antenna is actually an antenna pair (separate transmit and receive antennas), wherein each antenna exhibits high efficiency, small size and narrow bandwidth, with a frequency response that reduces (or eliminates) the need for additional filtering in the RF front-end. Such an antenna pair would reject undesired interferers with a minimum degradation of the desired SNR. Furthermore, the antenna pair would reduce the need for additional analog filtering in the RF front end, reducing the size, cost and power requirements of the handset. Thus, multi-band radios could be achieved by making the antenna pair reconfigurable, and controlling the antenna configuration using an antenna control unit (ACU) that receives commands from the radio's DSP. Following are measured and simulated results of some example reconfigurable antennas.

## 2. RECONFIGURABLE ANTENNA IMPLEMENTATION

### 2.1 Shorted Patch Antennas

A shorted patch antenna (SPA) is a good candidate to realize high efficiencies in a small form factor. Figure 2 shows a copper SPA fed by a coax. The SPA is about a quarter wavelength long at the fundamental resonant frequency, which can be reduced by adding a capacitor across the main radiating edge. Changing the value of this capacitor effectively tunes the antenna. An equivalent circuit model is used to optimize efficiency, bandwidth, and the design of a tuning circuit. The equivalent circuit of Figure 2 includes an inductor to model the feed probe and a resistor to account for copper losses. The transmission line section has the effective length of the radiating patch and is shorted on one end. The end opposite the short is loaded with a tuning capacitor to reduce the resonant frequency. A transformer to free space impedance accounts for the radiation resistance. The circuit model was derived and validated by comparing calculated input impedance to that measured on prototype SPAs of various sizes.

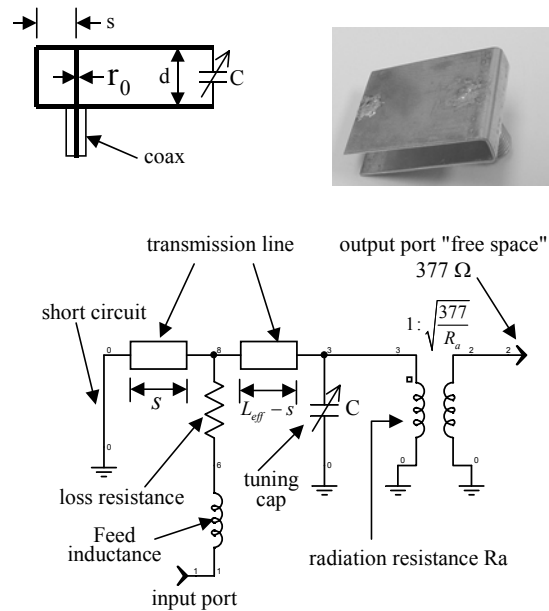


Figure 2. SPA drawing, hardware, and circuit model.

It is necessary to model the antenna as a two-port device to account for the effect of its frequency response on the system. It is shown in [3] that the transfer function of the antenna is equal to its total efficiency, which includes mismatch loss. Conductor loss and tuning circuit loss contribute to reduced efficiency and also affect the bandwidth. This two-port equivalent circuit of the SPA is invaluable for calculating the practical limitations on bandwidth, size, and efficiency and for determining the effects that losses in the tuning circuits have on these quantities.

Figure 3 shows typical efficiency versus frequency curves resulting from the circuit model for a SPA of dimensions 25 x 19 x 6 mm and loaded with 2.5 pF capacitors of different  $Q$  (loss). In a more complex tunable antenna system, additional capacitors are switched in and out of the circuit. Nevertheless, the overall capacitance and tuning circuit loss resistance may be lumped into a single lossy capacitor loading the end of the SPA in order to study the effects on efficiency. As the  $Q$  of the tuning circuit is decreased from 1000 to 250, the peak efficiency drops by 3 dB. From the circuit model, it was observed that the losses in the tuning circuit reduce efficiency more than conductor losses do. Thus it is important that the tuning circuit (including switches) must have very low losses.

Figure 4 shows the relationship between tuning circuit  $Q$ , footprint, efficiency, and bandwidth for an

antenna with a fixed resonant frequency (850 MHz) and

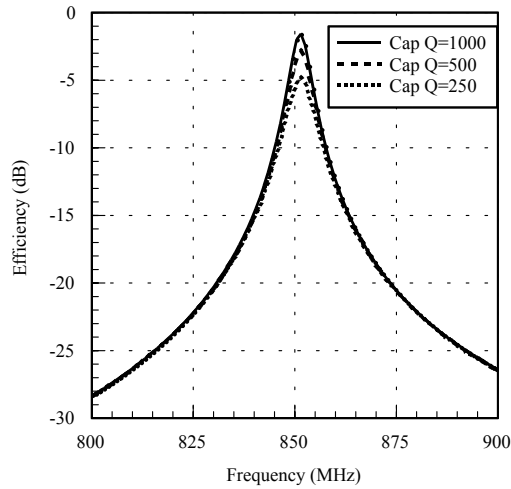


Figure 3. Calculated efficiency of SPA loaded with capacitors of various Q

height (5 mm). As the footprint is decreased, very high  $Q$ s are needed to achieve even modest efficiencies. For a 20mm footprint, circuits with  $Q$ s of 150 are needed to obtain a 12 to 15 MHz antenna bandwidth, which could cover each of the GSM bands in 3 to 4 steps with radiation efficiencies of 20 to 30%.

As the frequency increases, the efficiency curves move to the right of the graph and the bandwidth curves move toward the bottom left corner. Thus, for higher frequencies, the challenges exposed in Figure 4 for 850 MHz become somewhat less harsh.

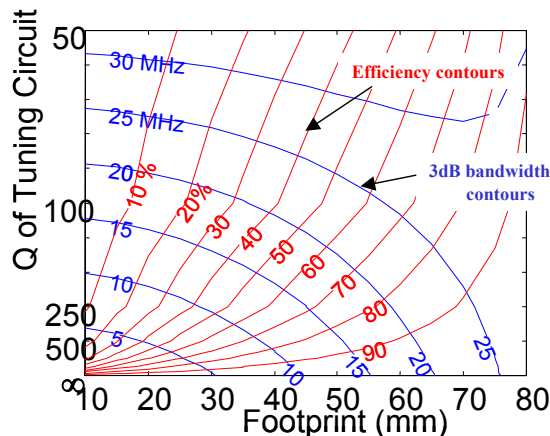


Figure 4. Contours of efficiency and bandwidth at 850 MHz versus antenna size (footprint) and tuning circuit  $Q$  for square SPA of height 5 mm.

Another effect that is more difficult to calculate is the proximity of external lossy objects like a human

operator's head or hand. These decrease the efficiency and, in some cases, de-tune the antenna. Compensation for the latter effect is possible with a tunable antenna. These phenomena may be quantified through measurements.

## 2.2 Dual Tunable SPA Hardware Demonstration

The hardware shown in Figure 5 was assembled in order to demonstrate a tunable Tx/Rx SPA pair for the GSM 850 MHz and 900 MHz bands. The Tx SPA is larger so that efficiency is maximized for transmit. Each antenna has two loading capacitors. The first capacitor allows each electrically small antenna ( $\sim 0.07\lambda$ ) to be resonant in the 900 MHz band. Coverage of the 850 MHz band is accomplished by switching a second capacitor within the antenna aperture using a PIN diode and 3V battery.

These antennas were mounted on a 4 cm x 10 cm test ground plane and their efficiencies were measured in a Satimo spherical near field range [4]. In order to quantify the in-situ performance, the antenna efficiency was measured in the presence of the phantom head and hand shown in Figure 6.

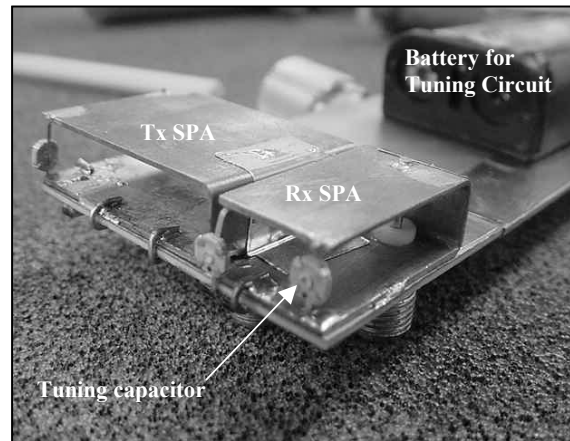


Figure 5. Cell/GSM SPA pair on evaluation board.

The efficiency-bandwidth product for each antenna in each band was computed for both free space and in-situ measurements. These data points are plotted in Figure 1 for comparison with the theoretical curves. The peak efficiencies measured in free space and in-situ for the smaller (Rx) antenna were almost equal. This is attributed to the fact that the radiating aperture of this antenna faced away from the hand. The radiating aperture of the Tx antenna was in closer proximity to the hand. As a result, this antenna had significantly lower efficiency in-situ. Nevertheless, all data points for these antennas are close

to the theoretical limit for a thin dipole antenna. Data points for a PCS antenna in free space with dimensions similar to the Tx antenna are displayed in Figure 1 as well.



Figure 6. In-situ evaluation of handset performance.

The in-situ efficiency versus frequency curves for each tunable antenna are plotted in Figure 7. In summary, we achieved 10 – 15 MHz of bandwidth, 30-40 % free space efficiency, and 15% in-situ efficiency with the Tx antenna that had approximately 3000 mm<sup>3</sup> volume. Similar bandwidth and in-situ efficiency were obtained for the 1500 mm<sup>3</sup> Rx antenna with its aperture orthogonal to the Tx antenna. To determine if the PIN diode switch was causing excessive loss, we simulated a perfect switch with an open circuit or shorting wire. The free space efficiency measured for this case via a Wheeler cap technique was found to be 50% for Tx and 20% for Rx. Obviously, better switches (such as MEMS switches) would result in

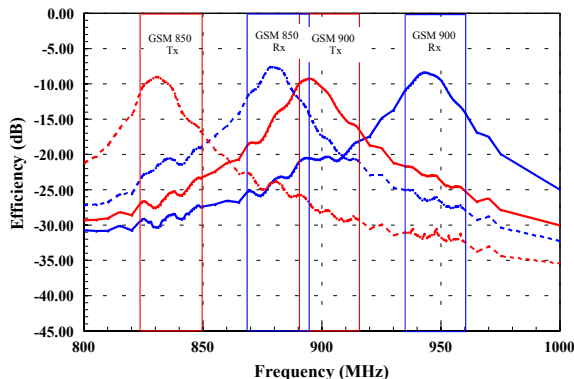


Figure 7. In-Situ measured efficiency (800 – 1000 MHz).

efficiency levels between that measured for the PIN diodes and short/open wire. Another important result is the coupling between antennas. The maximum coupling between the Tx and Rx antennas of this demonstration was -20 dB.

We have shown that antenna  $Q$ s of 50 to 100 are achievable in practice that result in bandwidths of 10 to 15 MHz at the Cell/GSM bands and 30 to 40 MHz at the PCS/DCS bands. Since the GSM Tx band is 25MHz at 900 MHz and the Rx band is 25MHz at 950MHz, 3 or 4 tuning states are required to cover each of these bands. The instantaneous bandwidth broadens as frequency increases, but up to a dozen states may be necessary to cover Cell, GSM, PCS, DCS and UMTS with one antenna. The addition of more switches and tuning states will degrade efficiency for the lowest frequency band of interest.

### 2.3 System Performance with a Tunable Antenna

Noting that the efficiency curve of the SPA resembles the frequency response of a bandpass filter, we became interested in determining if the frequency responses of the Tx/Rx antennas could be used to eliminate, or reduce the requirements on the RF filters required in a wireless transceiver. Separate Tx and Rx antennas might also allow for the elimination of a T/R switch or duplex filter if enough isolation can be achieved between PA output and LNA input. To test this hypothesis, we obtained a commercial PCS band handset, removed its external antenna, T/R switch and harmonic suppression filter, and put a Tx/Rx SPA pair that fit inside the handset enclosure, as illustrated in Figure 8. This phone was placed in a call box and tested in a PCS mode. The antennas were fixed to center frequencies of the GSM 1900 Tx and Rx bands and exhibited excellent performance using the center channels. Ultimately, a control signal is needed from the radio's

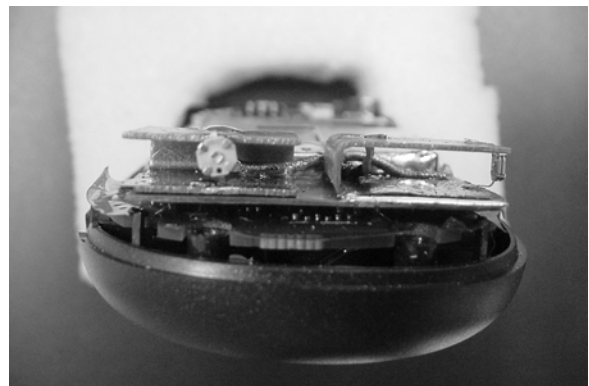


Figure 8. PCS handset with internal SPA pair.

baseband processor to configure the tuning circuit for operation in the proper frequency band.

In order to quantify the filtering robustness of the antenna, we performed a system simulation (using Elanix's System View software) to analyze system performance for both a conventional RF system architecture and a proposed RF system architecture based on the tunable SPA Tx/Rx pair. The specific configuration we analyzed comprises a full duplex (AMPS/CDMA), dual-band (US Cellular and US PCS band) superheterodyne receiver. The results discussed here were obtained for the US PCS band. We attempted to mimic the performance of off-the-shelf passive and active devices in our simulations. A block diagram of the conventional dual-band, full-duplex front-end is shown in Figure 9. The simulated portion of the system is indicated in the figure. A block diagram of a dual-band, full-duplex front-end based on the SPA pair is shown in Figure 10.

The results of the simulations are summarized in Table 1. As can be seen, the SPA-pair architecture offers almost the same image rejection as the conventional

SPA-pair architecture is substantially lower than that of the conventional architecture.

Table 1. Comparison of simulated results of conventional and SPA-pair front end architectures.

	Conventional	SPA Pair
Signal at Antenna		
Desired signal	-90 dBm	-90 dBm
Image at 200 MHz offset	-60 dBm	-60 dBm
Signal at mixer input		
Desired signal	-80.4 dBm	-79.2 dBm
Image at 200 MHz offset	-144 dBm	-140 dBm
Cascaded gain	9.6 dB	11.8 dB
Image rejection	84 dB	80 dB
System noise figure	4.3 dB	2.3 dB

### 3. CONCLUSIONS

We have demonstrated some state-of-the-art results for reconfigurable antennas that are suitable for internal installation in mobile wireless products. Separating the antennas into a Tx and Rx unit offers the flexibility to impedance match each one separately, thus eliminating separate matching network components on the board. Also, a T/R switch or duplex filter may be eliminated if enough isolation can be achieved between the antenna pairs. As one makes the antenna smaller, the available 3dB bandwidth shrinks if one desires to maintain the efficiency. Thus, a tuning network is necessary that must be controlled by the radio's baseband processor. This complexity is minimal if open loop control is sufficient. It is also possible to cover a large range, say 800MHz to 2 GHz with a single Tx/Rx antenna pair. The key to achieving a successful tuning circuit is to implement a switched bank of high  $Q$  capacitors with very low loss, which is a good application for MEMS switches.

### 4. REFERENCES

- [1] R.F. Harrington, "Effect of antenna size on gain, bandwidth and efficiency", Journal of Research of the NBS-D, Vol 64D, No. 1, Jan-Feb 1960.
- [2] D.T. Auckland, "Some observations on gain, bandwidth and efficiency of circular apertures", Atlantic Aerospace Technical Note, 27 Oct 94.
- [3] S.D. Rogers, et al., "Two-Port Model of an Antenna for Use in Characterizing Wireless Communications Systems Obtained Using Efficiency Measurements", *Digest of 2002 IEEE Antennas and Propagation Society Symposium*, San Antonio, TX, June 2002.
- [4] P.O. Iversen, et al., "Real-Time Spherical Near-Field Handset Antenna Measurements," *IEEE Antennas and Propagation Magazine*, vol. 43, no. 3, pp. 90-94, June 2001.

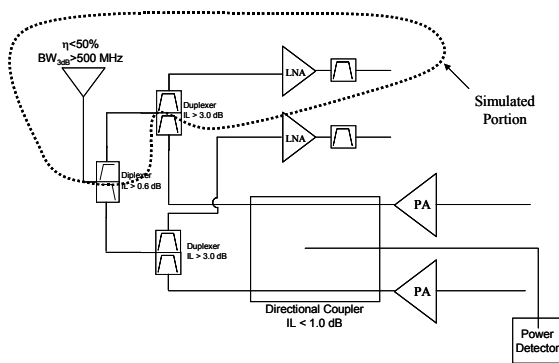


Figure 9. Conventional dual-band full-duplex front end.

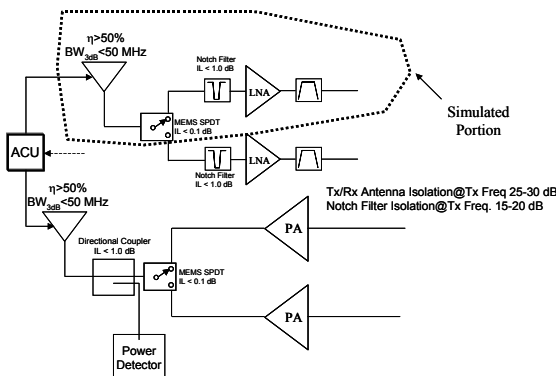


Figure 10. SPA-pair dual-band full-duplex front-end.

architecture while providing substantially better noise figure. Furthermore, the component count and cost of the